Proceedings of the 10th International Conference on Civil Structural and Transportation Engineering (ICCSTE 2025)
July, 2025 | Imperial College London Conference Center, London, United Kingdom
Paper No. 285
DOI: 10.11159/iccste25.285

Comparison of the Influence of Different Soil-Structure Interaction Models in a Five-Story Building on Soft Soil

Luis Izarra[1], Gustavo Loza[2], Gram Rivas[3]
[1]Peruvian University of Applied Sciences
Marina Avenue 2810, Lima, Peru
U20201B415@upc.edu.pe; U20201C178@upc.edu.pe
pccigrri@upc,edu.pe - London Conference Centre

Abstract **-** A comparative analysis will be carried out on the influence that four soil-structure interaction models have on the seismic performance of a five-story dual building composed of frames, reinforced concrete walls and isolated footings type foundations, whose initial premise states that these foundations are completely embedded in the ground. The methodologies selected for the comparison will be the D. D. Barkan - O. A. Savinov model, the A. E. Sargsian model, the model proposed by the Russian Standard SNIP 2.02.05-87 and the model proposed by the FEMA P-2091 manual in its sixth chapter. The data obtained from different measurement indicators will be compared, such as structural drifts, fundamental period, base shear, axial forces acting on a critical column and moments in a critical beam. At the end of the analysis, it was concluded that the SSI model that provides results that are most in line with Peruvian reality without the need to exaggerate the results is the one proposed by the FEMA manual, which represents a good precedent in favor of including the phenomenon in the Peruvian regulations.

Keywords**:** Soil-Structure Interaction, Seismic Analysis, Dual Structure, Reinforced concrete, Isolated Footing, FEMA manual.

1. Introduction

Seismic risk in Latin America is significant due to the high seismic danger of the region and issues like informal construction, especially in Peru, where the absence of a seismic-resistant design standard before 1997 and rapid population growth exacerbate the problem [1][2]. Considering soil-structure interaction (SSI) is essential, as Peruvian soils are not entirely rigid, which affects seismic performance, particularly on flexible soils [3][4]. However, the Peruvian E-030 standard does not address this phenomenon.

Various models integrate SSI into structures. For instance, a fixed-base model equivalent to a dynamic one effectively represents seismic amplifications [5]. Another improves an existing model, increasing the period by 6% [6]. Studies on dual buildings with basements reveal basal shear increases of up to 220% [7], and other research highlights the greater impact of SSI on soft soils [8].

This article evaluates four dynamic SSI models: the Barkan-Savinov model, the Sargsian model, the Russian Standard SNIP 2.02.05-87 [9], and the FEMA P-2091 model [10], selecting the most suitable for Peru. These models will be integrated into a reinforced concrete building with a dual system of frames and shear walls, supported on isolated footings over a flexible type E soil (IBC/ASCE 7) or S3 soil (Peruvian regulations). Using spectral modal seismic analysis, parameters such as story drifts, fundamental period, basal shear, axial forces, and displacements will be compared.

Notable differences arise due to the age of three models (Barkan-Savinov, Sargsian, and Russian Standard) and their omission of necessary parameters compared to the more recent FEMA model, which accounts for all six degrees of freedom (DOF). For instance, the Barkan and Sargsian models restrict rotation on the Z axis, unlike the Russian Standard and FEMA models. This comparison is critical since Peruvian regulations omit SSI despite the prevalence of flexible soils, providing a precedent for its inclusion and suggesting a validated model for structural analysis.

2. Methodology

The research method involves a comparative study of parameters obtained from the spectral modal seismic analysis of the structure. This comparison will identify which SSI model best represents the soil's influence on structural behaviour.

Variations between the four models and the embedded base model will be analysed, selecting the model that shows the most significant variation.

2.1. Method for research

For the object of study, which is a five-story reinforced concrete building with isolated footings, the superstructure had to be designed in accordance with the Peruvian E-030 Earthquake Resistant Design standard. This is essential because all models have, among others, the dimensions of the foundations as dependent variables. To obtain the size of the footings, it is necessary to complete the superstructure and continue with the design of the infrastructure. In addition, a soil mechanics test (SMT) of the stratum where the building will be located is required, not only for the design of the footings, but also certain parameters necessary to apply the equations that each methodology has.

2.2. Tools and manuals

The research utilized Etabs v.22 as the primary software for building design, structural and seismic analysis, and integrating the four SSI models to obtain and compare parameters. Microsoft Excel was essential for quantifying the equations representing the SSI phenomenon based on each methodology. The structural design process is not detailed in this article, as it is assumed that the superstructure and infrastructure are properly designed and validated by a specialist.

Three SSI models—D. D. Barkan-O. A. Savinov, A. E. Sargsian, and the Russian Standard SNIP 2.02.05-87—are quantified in the book "Seismic Interaction Soil-Structure in Buildings with Isolated Footings" by PhD. Ing. Genner Villarreal [9]. The FEMA P-2091 model [10] is formulated in the NIST GCR 12-917-21 manual, frequently cited by FEMA [11].

In Etabs, the phenomenon is represented by calculating the stiffness of Winkler springs, which model the six DOF, allowing soil displacements and rotations at each isolated footing in the coordinate axes.

3. Formulation Of Models

Each SSI model allows the calculation of the stiffnesses of the springs explained above that represent DOF and, depending on the methodology, we will obtain five stiffnesses for the models that allow 5 DOF, or six stiffnesses for those that allow 6 DOF. For the present article, only the formulas of the FEMA P-2091 manual proposal will be explained; the other proposals are explained in the cited book by engineer Villarreal.

The input data are the inertias of the rectangular footings, normalized to be calculated at the centroid of the acting faces. Equations (1) and (2) write the formulas.

$$I_{x;y} = \frac{bh^3}{12} \tag{1}$$

$$I_z = I_x + I_y \tag{2}$$

In the equations:

b: Perpendicular length of the studied axis of the rectangular area of the footing.

h: Length parallel to the studied axis of the rectangular area of the footing.

In addition to this, other soil characteristics are required that will be detailed later, which are obtained from an SMT.

3.1. Model proposed by FEMA P-2091

The methodology in the FEMA P-2091 manual references the NIST GCR manual, which compiles two SSI models: one by Pais and Kausel (1998) and another by Gazetas (1996) and Mylonakis et al. (2006), both representing the same SSI model [11]. These models account for six degrees of freedom and various soil parameters, with a single adjustment factor for static conditions for a rigid footing on flexible soil [10]. However, only the Gazetas and Mylonakis model is used for comparison due to its more recent development (2006) and its inclusion of additional parameters, such as moments of inertia in X and Y and the polar moment of the footing area, making it more comprehensive. Equation (28), (29), (30), (31), (32) and (33) describe the methodology proposed by Gazetas and Mylonakis with the readjustment factor.

$$K_{z,sur} = \frac{2\frac{E}{2\,(1+v)}L}{1-v}\left(0.73+1.54\left(\frac{B}{L}\right)^{0.75}\right)\left(1+\frac{D}{21B}\left(1+1.3\frac{B}{L}\right)\right)\left(1+0.2\left(\frac{A_w}{4BL}\right)^{\frac{2}{3}}\right) \quad (3)$$

$$K_{y,sur} = \frac{2\frac{E}{2\,(1+v)}L}{2-v}\left(2+2.5\left(\frac{B}{L}\right)^{0.85}\right)\left(1+0.15\sqrt{\frac{D}{B}}\right)\left(1+0.52\left(\frac{z_w A_w}{BL^2}\right)^{0.4}\right) \quad (4)$$

$$K_{x,sur} = \left((K_{y,sur} - \frac{0.2}{0.75-v}\frac{E}{2\,(1+v)}L\left(1-\frac{B}{L}\right)\right)\left(1+0.15\sqrt{\frac{D}{B}}\right)\left(1+0.52\left(\frac{z_w A_w}{LB^2}\right)^{0.4}\right) \quad (5)$$

$$K_{zz,sur} = \frac{E}{2\,(1+v)}J_t^{0.75}\left(4+11\left(1-\frac{B}{L}\right)^{10}\right)\left(1+1.4\left(1+\frac{B}{L}\right)\left(\frac{d_w}{B}\right)^{0.9}\right) \quad (6)$$

$$K_{yy,sur} = \frac{\frac{E}{2\,(1+v)}}{1-v}\left(I_y\right)^{0.75}\left(3\left(\frac{L}{B}\right)^{0.15}\right)\left(1+0.92\left(\frac{d_w}{B}\right)^{0.6}\left(1.5+\left(\frac{d_w}{D}\right)^{1.9}\left(\frac{B}{L}\right)-0.6\right)\right) \quad (7)$$

$$K_{xx,sur} = \frac{\frac{E}{2\,(1+v)}}{1-v}\left(I_x\right)^{0.75}\left(\frac{L}{B}\right)^{0.25}\left(2.4+0.5\left(\frac{B}{L}\right)\right)\left(\eta_{xx}=1+1.26\frac{d_w}{B}\left(1+\frac{d_w}{B}\left(\frac{d_w}{D}\right)-0.2\sqrt{\frac{B}{L}}\right)\right) \quad (8)$$

For both models, the variables used are the following:
Kx;y;z: Translation in the coordinate axes (tnf/m).
Kzz: Torsion in the Z axis (tnf-m).
Kxx;yy: Swing on the X and Y axes (tnf-m).
B: Half the length of the footing parallel to the Y axis (m).
L: Half the length of the footing parallel to the X axis (m)
v: Poisson's modulus of the soil.
Jt: Equivalent to the inertia Iz, summation of the inertias Ix with Iy (m4).
D: Depth of bottom of footing (m).
dw: Depth of footing (m).
Zw: Distance from the surface ground to half of the depth of the footing (m).
Aw: Lateral area of the footing (m).
E: Soil modulus of elasticity (tnf/m2).

4. Analysis And Validation

The building has 25 footings, some of which have the same dimensions, which reduces the number to 20 geometrically equal footings. For the calculations, we require the soil conditions where they are located. Table 1 organizes these conditions in summary form.

Table 1: Soil Conditions

Parameter	Value	Unit
Type of soil	S3	
Modulus of elasticity	500	Effort (tnf/m2)
Poisson's ratio	0.25	Dimensionless

Parameter	Value	Unit
Specific weight	1.6	Weight density (tnf/m3)
Shear Modulus	200	Effort (tnf/m2)

To summarize the calculations performed, we will work with the Z-1 footing, whose dimensions are (2.05x1.95x0.40) meters, and it also receives from the building a CV of 7.50 tnf and a CM of 41.73 tnf.

Furthermore, since the four SSI models are described in detail, the calculation of the spring stiffnesses will not be explained, and the article will be limited to presenting the results of each method. Table 2 organizes the results of the translation and rotation spring stiffnesses for the Z-1 footing.

Table 2: Stiffness Coefficients for Translation Of Z-1

Model of SSI	Spring stiffness					
	Translation in X (K_x)	Translation in Y (K_y)	Translation in Z (K_z)	X Swing (K_{xx})	Y Swing (K_{yy})	Z Torsion (K_{zz})
Barkan	69380.239	69380.239	80943.613	289171986	261648180.3	-
Sargsian	687.335	687.335	1536.134	897.541	812.111	-
Norma Rusa	4334.433	4334.433	6192.047	4337.013	3924.210	4130.611
FEMA	2347.515	2334.186	1651.003	1785.169	1783.943	3714.692

After integrating the SSI, it is necessary to compare the structural response of the building against the embedded model and verify the variation offered by each proposal to subsequently choose the most balanced one. For the springs in the plate supports, the theory of parallel springs was used [13].

4.1. Comparison of Drifts

The structure drifts are perhaps the main indicator of the influence of the SSI on the structure, in this case, the drifts were divided into the “X” and “Y” directions for a better analysis. Fig. 1 shows the variation of drifts on the “X” axis.

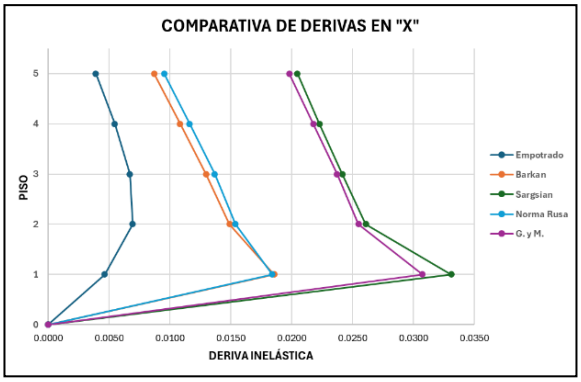

Fig. 1: Comparison of inelastic drifts on the “X” axis

Likewise, Fig. 2 shows the variation of drifts on the “Y” axis.

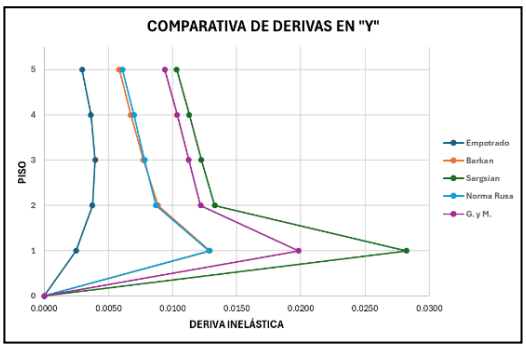

Fig. 2: Comparison of inelastic drifts on the "Y" axis

In the X axis, the SSI phenomenon significantly influences drifts, with the embedded base model showing the lowest values. Drifts increase as models change due to base movement and rotation, with the Barkan model showing the smallest increase, followed by the Russian Standard, the Gazetas and Mylonakis model, and the Sargsian model, which produces the highest drifts. The Sargsian model, being simplified and academic, has lower spring stiffness, leading to exaggerated responses, and it restricts rotation on the Z axis, making it less realistic for ground behaviour.

For the Y axis, the Sargsian model also shows exaggerated results like the X axis, with significant variation from the embedded base. Another study reported drift increases of up to 1246.67% on the X axis and 1057.14% on the Y axis for buildings on soft soil [12].

The FEMA P-2091 model appears most reliable, allowing substantial but coherent variations without exaggeration. Its focus on the shear modulus, which is low for flexible soils, results in appropriately small stiffness values.

4.2. Comparison of Vibration Periods

Comparing vibration periods is important because it allows us to know how long it takes for the building to oscillate. It is also a good indicator of the flexibility or rigidity of the structure. Fig. 3 shows the variation of the fundamental period for each SSI model.

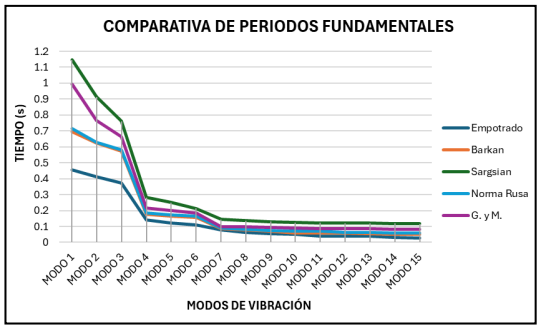

Fig. 3: Comparison of Vibration Periods

The Sargsian model exaggerates seismic analysis results, while the Barkan and Russian Standard models show consistent and closely related values. The FEMA manual model remains the most coherent, admitting six DOFs without exaggerating results like the Sargsian model. Vibration periods align from Mode 4 onward, with the first three modes considered "fundamental" due to their criticality.

The ascending order of vibration periods is embedded base (lowest values), followed by the Barkan model, then the Russian Standard model (very close to Barkan), the Gazetas and Mylonakis model, and finally, the Sargsian model with the highest values.

4.3. Comparison of Basal Shears

For the example of the building, the base shears were calculated with the dynamic earthquake divided into the two axes "X" and "Y". Fig. 4 shows the variation of the base shears of the building for each SSI model and for each type of earthquake.

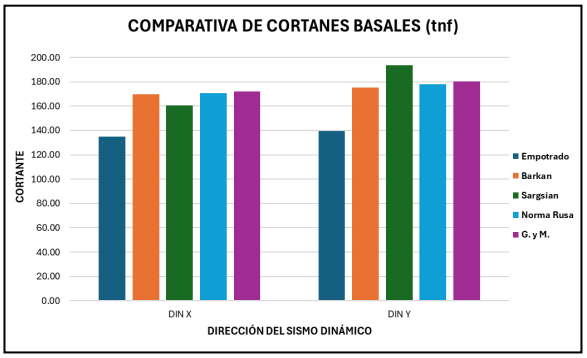

Fig. 4: Comparison of Basal Shears

The basal shear obtained with all models shows an increase, which may seem contradictory since longer periods usually reduce accelerations and basal shears. However, this increase can be attributed to soft soil and real earthquakes, where the acceleration spectrum peaks at intermediate-long periods, amplifying inertial forces [15].

All SSI models yield basal shear values between 165-180 tnf. However, the Sargsian model shows inconsistencies, with lower basal shear on the X axis but higher on the Y axis compared to the others. The remaining models maintain consistent values across axes, notably the Russian Standard and FEMA manual models, which present similar and reliable results.

Overall, all models, except the Sargsian model, produce consistent results, making the latter suitable only for reference and not definitive conclusions.

4.4. Comparison of axial loads in critical column

Fig. 5 compares the values of this load acting on a column.

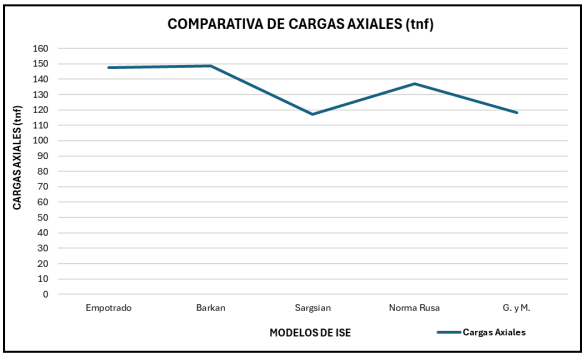

Fig. 5: Comparison of axial loads in critical column

The axial loads on the critical column decrease with three of the four SSI models, except for the Barkan model, which shows a slight increase. This reduction occurs because soil-structure interaction alters the dynamic behavior of the structure, allowing the soil to absorb part of the seismic forces, reducing the loads transmitted to the columns. The soil's deformation acts as a shock absorber, redistributing loads and relieving tension on critical columns.

The Barkan model, with very high spring stiffness and only five DOFs (restricting rotation on the Z axis), does not allow sufficient deformation for the soil to act effectively as a shock absorber. This effect is directly linked to the stiffness of the spring representing translation on the Z axis; lower stiffness enhances the shock absorber effect.

Overall, except for the Barkan model, the other models produce consistent results. The Barkan model should be considered only as a reference, while the FEMA model remains the most reliable and consistent across parameters.

4.5. Comparison of moments in critical beam

It is necessary to evaluate the moments present in the critical beam, since these are the moments with which the steel design is made. Fig. 6 shows the comparison of the moments of the beams offered by each SSI model.

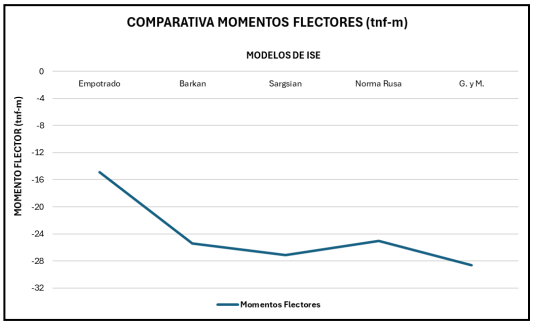

Fig. 5: Comparison of moments in critical beam

In order to interpret the bending moments, it must be understood that the importance lies in the magnitude of the moment, and not so much in the sign that only indicates the position where it acts. Therefore, despite meaning a “reduction” in terms of relative values, this is not entirely beneficial. The beam is supporting moments much greater than those that appear with the embedded base model, so a redesign is necessary.

Analyzing the values provided by each model, the most critical bending moment is obtained in the Gazetas and Mylonakis model, which is consistent with what is expected since, by admitting rotations in the three coordinated axes, the columns tend to experience additional displacements, which leads to the beams experiencing an increase in the bending moments. Another reason that explains this increase is the different distribution of loads in the building due to the integrated phenomenon. It cannot be considered that it exaggerates the moments because, compared to the other models, the quantities are very close.

This model is followed by the one proposed by Sargsian, then the Barkan model and finally the proposal of the Russian Standard as the model that, among the others, increases the bending moments of the critical beam to a lesser extent.

4. Conclusion

The model that best represents the deformations that the soil undergoes and the phenomenon of soil-structure interaction is the one proposed by the FEMA P-2091 manual, because it represents a much more recent model than the previously mentioned ones, in addition to the fact that it includes six DOF in its methodology, which implies that it admits in a more realistic way the types of variations that the foundations of the building undergo due to soil deformations. Another important point is that it admits many more parameters than other models, such as the shear modulus, which is a property that indicates the capacity of the soil to withstand shear stresses. Complementing all this, the values provided by the model are expected from the literature studied, without exaggerating results and maintaining coherence with each value provided by the model.

On the other hand, the model that should be taken as a reference criterion is the one proposed by A. E. Sargsian, because, when considering very small stiffness values in contrast to the other models, the effects are amplified in an exaggerated manner and far from showing realism in its responses, it ends up providing reference values only for a precise analysis of SSI.

Acknowledgements

A la Dirección de Investigación de la Universidad Peruana de Ciencias Aplicadas por el apoyo bridado para realización de este trabajo de investigación a través del incentivo UPC-EXPOST-2024-2.

References

[1] I. Velásquez, “Estudio comparativo del comportamiento estructural de un edificio de 06 niveles considerando 03 modelos dinámicos en la interacción suelo estructura – Lima 2022”, Tesis de Título Profesional de Ingeniería Civil, Universidad Tecnológica del Perú, 2022. Disponible en: https://hdl.handle.net/20.500.12867/7593

[2] R. Fassabi, “Análisis de vulnerabilidad física para la prevención del riesgo sísmico en el AH Lomo de Corvina, Villa El Salvador, Lima – 2021”, Tesis de Magister en Ingeniería Civil, Pontificia Universidad Católica del Perú, 2021. Disponible en: https://tesis.pucp.edu.pe/repositorio/bitstream/handle/20.500.12404/23060/FASSABI_RUIZ_MARCO_ANALISIS_VULNERABILIDAD_FISICA.pdf?sequence=1&isAllowed=y

[3] M. Brahimi y Y. Menasri, "Assessment of the effects of soil-structure interaction on the seismic response of the RC frame buildings by developing seismic fragility curves based on SPO2IDA analysis," *Journal of Applied Science and Engineering*, vol. 27, no. 2, pp. 2075–2085, 2023. DOI: 10.6180/jase.202402_27(2).0009

[4] J. Córdova y A. Godier, “Análisis y evaluación de la interacción suelo–estructura (ISE) mediante una comparación de diseño convencional y un modelo integrado de un edificio comercial de 7 pisos con un sistema dual en la ciudad de Pucallpa–Ucayali”, Tesis de Titulación en Ingeniería Civil, Universidad Nacional de Ucayali, 2018. Disponible en: http://repositorio.unu.edu.pe/handle/UNU/4094

[5] D. Forcellini, "A novel framework to assess soil-structure interaction (SSI) effects with equivalent fixed-based models," *Applied Sciences*, vol. 11, no. 21, p. 10472, 2021. DOI: 10.3390/app112110472

[6] J. Li, M. Chen, y Z. Li, "Improved soil–structure interaction model considering time-lag effect," *Computers and Geotechnics*, vol. 148, p. 104835, 2022. DOI: 10.1016/j.compgeo.2022.104835

[7] F. Ayala, E. Sáez, y C. Magna-Verdugo, "Computational modelling of dynamic soil-structure interaction in shear wall buildings with basements in medium stiffness sandy soils using a subdomain spectral element approach calibrated by micro-vibrations," *Engineering Structures*, vol. 252, p. 113668, 2022. DOI: 10.1016/j.engstruct.2021.113668

[8] J. Wang, T. Guo, Y. Xie, y Z. Du, "Parametric analyses of dynamic interaction between three-dimensional soil and frame structure group under earthquake loadings," *Bulletin of Earthquake Engineering*, vol. 20, no. 15, pp. 8305–8324, 2022. DOI: 10.1007/s10518-022-01511-y

[9] G. Villarreal, Interacción sísmica suelo-estructura en edificaciones con zapatas aisladas, Lima – Perú, 2009. Disponible en: http://blog.pucp.edu.pe/blog/wp-content/uploads/sites/109/2009/07/Interaccion-suelo-zapata.pdf

[10] Federal Emergency Management Agency, FEMA P-2091: A Practical Guide to Soil-Structure Interaction, 2020. Disponible en: https://www.atcouncil.org/docman/fema/298-fema-p-2091-soil-structure-interaction/file

[11] National Institute of Standards and Technology, Soil-structure interaction for building structures (NIST GCR 12-917-21), U.S. Department of Commerce, 2012. Disponible en: https://www.nehrp.gov/pdf/nistgcr12-917-21.pdf

[12] J. Caño, Apuntes para una breve introducción a la Resistencia de Materiales y temas relacionados, Universidad de Valladolid, Escuela de Ingenierías Industriales, 2012. Disponible en: https://uvadoc.uva.es/handle/10324/2029

[13] F. P. Beer, E. R. Johnston Jr., J. T. DeWolf, y D. F. Mazurek, *Mechanics of materials*, 6th ed., McGraw-Hill Education, 2015

[14] J. Tasilla, Efecto de la interacción suelo–estructura en el comportamiento estructural, del sector "E" del Hospital Regional de Cajamarca considerando diferentes tipos de suelos, Cajamarca – 2017, Tesis de Título Profesional en Ingeniería Civil, Universidad Nacional de Cajamarca, 2018. Disponible en: https://repositorio.unc.edu.pe/handle/20.500.14074/2838

[15] American Society of Civil Engineers, Minimum design loads and associated criteria for buildings and other structures (ASCE/SEI 7-16), 2017. Disponible en: https://www.academia.edu/68636118/ASCE_7_16_MINIMUM_DESIGN_LOADS_2017_